International Conference on Space Optics—ICSO 1997

Toulouse, France

2–4 December 1997

Edited by George Otrio

Wavefront sensors for the active control of earth observation optical instruments

Marie-Thérèse Velluet, Vincent Michau, Gérard Rousset

International Conference on Space Optics — ICSO 1997, edited by Georges Otrio, Proc. of SPIE Vol. 10570, 105701D · © 1997 ESA and CNES · CCC code: 0277-786X/18/$18 · doi: 10.1117/12.2326489

WAVEFRONT SENSORS FOR THE ACTIVE CONTROL OF EARTH OBSERVATION OPTICAL INSTRUMENTS

Marie-Thérèse VELLUET, Vincent MICHAU, Gérard ROUSSET

Office National d'Études et de Recherches Aérospatiales
BP 72, 92322 Châtillon cedex
FRANCE

RESUME - En vue d'accroître leur résolution, les futurs instruments optiques d'observation de la Terre depuis l'espace nécessitent de grandes optiques. De ce fait, ils sont extrêmement sensibles aux déformations de la structure du télescope et des optiques elles-mêmes. Aussi, afin de maintenir le niveau de performance demandé pendant la durée de vie de l'instrument, le contrôle optique actif paraît une solution prometteuse. Ce contrôle passe par la mesure des aberrations du système optique. Nous présentons les différents analyseurs existant et indiquons leurs performances. Ceci est illustré à l'aide de résultats obtenus à l'ONERA par simulations numériques et expérimentations en laboratoire. La synthèse des caractéristiques spécifiques de chaque analyseur est effectuée en fonction des besoins (nature des défauts à corriger, fréquence de correction par exemple) et des contraintes apportés par les systèmes de contrôle actif (nature de la source, encombrement).

ABSTRACT - To enhance their accuracy, the future optical instruments for Earth observation from Space need larger optics. Consequently, they become extremely sensitive to the deformation of the telescope structure and of the optical elements themselves. To maintain the required performance level during the life of the instrument, the optical active control seems to be a promising solution. This control requires the measurement of the optical system aberrations. We present different Wave Front Sensor (WFS) concepts and give their performance which is illustrated by results obtained at ONERA from numerical simulations and laboratory experiments. The sensor main features are given according to requirements (aberration characteristics, correction frequency) and constraints brought by active control systems (source, overall dimensions).

1 - INTRODUCTION

To increase the resolution of new instruments for Earth observation from space larger optical systems are required. These instruments become more sensitive to the deformation of the telescope structure and of the large primary mirror. To maintain the required performance level along the instrument life time, an active control optical system seems to be a promising solution. It may also relax some design and manufacturing constraints, such as optical quality and thermal control, and in this way reduce the cost of the instrument.

The aim of this paper is to describe the WFS that can be useful for the control of these active optics systems. First, we list the main required specifications of WFS. From these requirements, we present three potential wavefront sensors: the Shack-Hartmann WFS which measures the local slopes of the wavefront, the curvature sensor which gives its local curvature and the phase diversity WFS which

estimates the wavefront from intensity distributions near the focus. The phase reconstruction process is discussed. The main errors in the phase determination are estimated.

2 - ACTIVE OPTICS CONCEPT

An active optics system is a servo-system able to correct in real time the instrument aberrations which can appear during its life time.

The active optics loop consists in measuring the aberrations, in computing in real time the correction to be applied and in compensating for the aberrations with the wavefront corrector devices.

The origin of the aberrations are the deformation of the structure and of the primary mirror.

The structure deformation can be measured directly from position or tilt sensors or indirectly from wavefront sensors that measure the aberrated wavefront. The main aberrations induced by the structure deformation are defocus and decentering astigmatism and coma. The wavefront measurement, directly related to image quality, provides an estimation of the actual performance of the system.

For Earth observation optical systems, the general specifications of the wavefront sensors are:
- to be used with terrestrial scenes which are extremely extended sources with limited brightness.
- to be highly stable along the instrument life time.
- to be designed for low order aberrations measurement which are the main sources of image degradation.
- to deliver high accuracy wavefront measurement (typically $\frac{\lambda}{50}$ rms) because of the wavefront error budget for such instruments.

3 - HOW TO SENSE THE WAVEFRONT ?

It is not possible at optical wavelength to measure directly the phase of the electromagnetic field. The detectors are only sensitive to intensity. Generally, indirect methods must be used in order to translate information related to the phase into intensity signals to be processed.

3.1 - Pupil plane techniques

Current wavefront sensing techniques are derived from methods used in optical testing. There are two classes of methods based on either interferometry or geometrical optics concepts. The first one uses the principle of coherent light beam superimposition to form interference fringes while the second one uses the property that the light rays are orthogonal to the wavefront.

In the optical shop, the interferometer is a well known instrument, like Fizeau interferometer: the optical path differences between the distorted wavefront and a reference plane are determined. But these sensors can only be used with coherent sources and require a reference arm. Their implementation in an active optics loop is relatively complex.

The second class of methods has also been well known since a long time for optical testing: e.g the Foucault knife and the Hartmann test[Mal 92] Since their principle is based on geometrical optics, all these sensors can be used with white light extended sources. More recently, two wavefront sensors became available: the Shack-Hartmann WFS , which measures the wavefront local slope, and the wavefront local curvature sensor.

3.2 - Focal plane techniques

The focal plane techniques are based on the estimation of the phase from the intensity distribution near the focal plane. For a monochromatic light point source, it is the point spread function (PSF) ($PSF = TF(P(\vec{r})\exp^{j\varphi(\vec{r})})^2$). $P(\vec{r})$ is the aperture function and $\varphi(\vec{r})$ is the optical aberration function. For an extended object, this intensity distribution is equal to the convolution of the object by the PSF.

The estimation of the phase is an inverse problem. It is called *phase retrieval*[Fie 82]. The Gershberg-Saxton iterative algorithm is a basic technique to solve this problem[Ger 71]. In general, there is no unique solution and multiple measurements must be used. Recent developments[Pax 92] were made in order to use a number of intensity distribution measurements encoded by known aberrations like defocus. It is called the *phase diversity*.

4 - THE MAIN WAVEFRONT SENSORS IN ACTIVE OPTICS

We have focused our works on three wavefront sensors: the Shack-Hartmann WFS , the phase diversity technique and the curvature sensor. Even if the curvature sensor can not yet be used with extremely extended source, it has the advantage of being easily implemented.

4.1 - The Shack-Hartmann wavefront sensor

4.1.1 - Principle

The principle of the Shack-Hartmann WFS is illustrated on Figure 1.

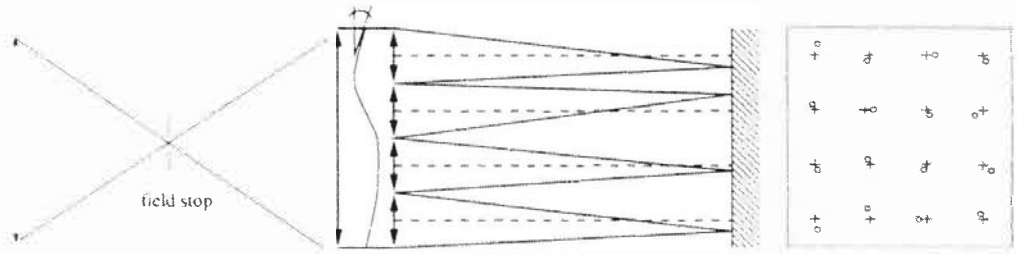

Fig. 1: Principle of the Shack-Hartmann wavefront sensor

A lenslet array, conjugated with the pupil plane of the instrument, samples the incoming wavefront. If the wavefront is plane, each lenslet forms an image of the source at its focus (crosses in Figure 1). If the wavefront is disturbed, each lenslet forms an image in an out of axis focus (circles in Figure 1).

The measurement of the image shift for each lenslet directly gives the local wavefront slope. It is performed by the computation of the center of gravity (C_x, C_y) of the image. For a limited extent source, it is related to the mean local wavefront slope by:

$$\frac{C_x}{F} = \frac{\lambda}{2\pi S_{sp}} \iint_{\text{subaperture}} \frac{\delta\varphi}{\delta x} dS \qquad (4.1)$$

where λ is the observation wavelength, S_{sp} the subaperture surface and F the focal length of the lenslet.

This sensor is compact and with no moving parts. An accurate calibration of the focus's position of the lenslet array requires a plane reference wavefront.

If the sensor is used with an extended source, the field stop size is chosen to avoid the overlap of the lenslet images. In that case the local wavefront slope is computed by a correlation method using a reference image. Figure 2 shows an image pattern of the Shack-Hartmann WFS used with an extended source.

The Shack-Hartmann WFS has been developed and used in ONERA for many years. In the case of point sources, the main application is the measurement of the wavefront residual error in an adaptive optics system in order to correct the turbulence degraded images. In the case of extended sources, we made laboratory experiments and validated the concept for active optics in space[Fon 92].

Fig. 2. Focal plane of the Shack-Hartmann WFS with an extended source

4.1.2 - Wavefront reconstruction

The wavefront is reconstructed from the slope measurements. The wavefront vector Φ is deduced from the measurement vector S of M elements (slopes in two directions) by the general relation: $\Phi = BS$. B is called the reconstruction matrix.

A number of techniques are available to compute B. Two classes are well identified in the literature: the zonal methods and the modal methods[Sou 80]. In the zonal methods, the phase is determined on a discrete set of points distributed over the telescope aperture. In the modal methods, the phase is expanded on a set of basic functions Z_i called the modes. We can expressed Φ by:

$$\Phi(\vec{r}) = \sum_i a_i Z_i(\vec{r}) \tag{4.2}$$

where the a_i are the expansion coefficients. In either case, least-square estimation is used for the phase reconstruction.

The incoming aberration vector Φ is related to the vector S by $S = A\Phi$. A is called the interaction matrix. Then to least mean square solution, B is equal to $(A^t A)^{-1} A^t$. Because, in active optics systems, we are just interested in low order aberrations, the modal reconstruction method is well adapted. The different terms of the matrix A are expressed by:

$$A_{ij}^x = \frac{1}{d^2} \iint_{\text{subaperture } j} \frac{\delta Z_i(\vec{r})}{\delta x} dS \text{ and } A_{ij}^y = \frac{1}{d^2} \iint_{\text{subaperture } j} \frac{\delta Z_i(\vec{r})}{\delta y} dS \tag{4.3}$$

where the Z_i can be the Zernike polynomials and d the subaperture diameter.

4.1.3 - Wavefront errors

The accuracy of the Shack-Hartmann WFS is mainly limited by three types of errors: the noise on the wavefront slope measurement which induces an error on the aberration estimation, the fitting error and the aliasing error.

The noise influence on the slope determination is expressed
- for a point source and pure photon noise by[Rou 93]

$$\sigma_\alpha^2 = \frac{1}{N_{ph}} \left(\frac{\pi d}{\lambda} \right)^2 \text{ (rd}^2\text{)} \tag{4.4}$$

where N_{ph} is the number of photoelectrons per subaperture and exposure time, α the angular size of the source image.

- for an extended source by[Fon 92]:

$$\sigma_\zeta^2 = \pi^2 \frac{m^2 \sigma_b^2}{n^2 \sigma_i^2} \text{ (rd}^2\text{)} \tag{4.5}$$

where m is the full width at half maximum of the image autocorrelation, n the width of the image used for the correlation, σ_b^2 the uniform noise per pixel (rms) and σ_i^2 the spatial variance in the reference image. Eq. (4.5) assumes a Shannon sampling of the images.

The noise from the measurements is propagated in the reconstruction process. By assuming that the slope errors are independent, uncorrelated and equal, the wavefront error σ_w^2 after reconstruction is:

$$\sigma_w^2 = \sum_i \sum_j B_{ij}^2 \sigma_\zeta^2 = trace(BB^t)\sigma_\zeta^2 \tag{4.6}$$

When a modal reconstruction is used, and for a Zernike expansion, the noise is essentially propagated on the low order aberrations following a $(n+1)^{-2}$ law where n is the Zernike radial degree[Rig 92]. We can write $\sigma_{a_i}^2 = k(n+1)^{-2}\sigma_\zeta^2$

The fitting error is the contribution of the high order aberrations which are not measured by the sensor. In the case of a modal reconstruction and for a Zernike expansion, the error σ_f^2 can be expressed in rd^2 by:

$$\sigma_f^2 = \sum_{N+1}^{\infty} a_i^2 \tag{4.7}$$

In an active optics system this error is essentially due to the residual aberrations after polishing of the optical components themselves.

Because the measurements are done on a finite grid (number of subapertures), aliasing of high order aberrations occurs (sampling theorem). This aliasing depends on the spatial spectrum of the measured wavefront and on the number of subapertures. To measure the aberrations due to the structure deformation, typically twenty subapertures seem to be enough. To correct the primary mirror deformation, the subaperture number will be higher and of the order of actuators number. Because the slope sensors are much more sensitive to low spatial frequencies the aliasing due to the sampling remains quite low.

4.2 - The phase diversity wavefront sensor

4.2.1 - Principle

Phase diversity WFS is based on the simultaneous measurement of two quasi monochromatic images. The first image is recorded in the focal plane of the optical system. The second image is recorded in an out of focus plane. The distance between these two planes is assumed to be known. The defocus introduces a quadratic phase diversity. The goal is to identify the object and the phase aberrations that are consistent with both collected images, given the known phase diversity. This technique works well with extended objects and even terrestrial scenes.

The phase diversity technique was first proposed by Gonsalves[Gon 82] to improve the quality of the aberration degraded images and then applied by several authors, particularly to ground-based solar imaging through atmospheric turbulence. In addition to the restoration of an aberration-free image, the phase diversity allows to determine the optical system aberrations. It was successfully applied to the determination of the Hubble Space Telescope aberrations[Rod 93, Fie 93].

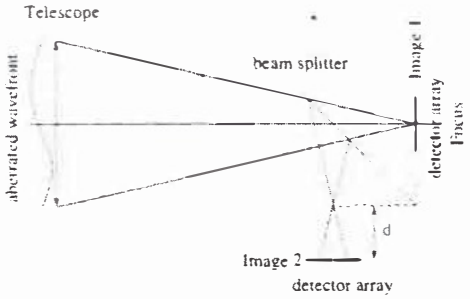

Fig. 3: Principle of the phase diversity sensor

The method of phase diversity offers several advantages. The optical hardware only requires a simple beam splitter and a second detector array as illustrated in Figure 3. Both recorded images I_1 and I_2 can be expressed as functions of the wavefront φ and of the source O by:

$$I_k = O * S_k \quad (k = 1, 2) \tag{4.8}$$

where S_k is the point spread function in the phase diverse plane k.

In the data reduction, the wavefront estimation from the measurements of the two images is performed by minimizing the distance E between the measured intensity distribution I_1 and I_2, and the estimated values of O and S. The error is expressed as:

$$E^2 = |I_1 - O_e * S_{e1}|^2 + |I_2 - O_e * S_{e2}|^2 \tag{4.9}$$

The subscript e denotes the current estimation in the iterative algorithm.

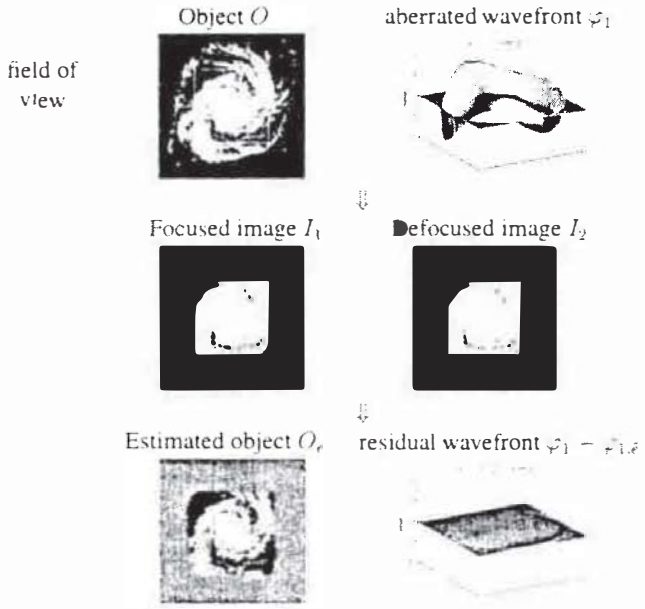

Fig. 4: Example of simulation with an extended source (galaxy M51)

To characterize the performance of phase diversity WFS, we have implemented and studied this method first by numerical simulations and second by laboratory experiments[Mey 97]. Figure 4 illustrates the simulation. The determination of the phase is very accurate: the residual method error between estimated and actual phases is less than $\frac{\lambda}{1500}$ rms.

4.2.2 - Wavefront errors

We have studied the influence of the photon noise in the images on the wavefront estimation accuracy using both analytical analysis and numerical simulations[Mey 97]. Assuming that the image noise statistics obey a Poisson law, we have shown that:
- the error is inversely proportional to the total flux level and to the pixel number in the images.
- The mean value of estimated Zernike expansion coefficients is not biased at high flux.

It is important to notice that the noise propagation on the Zernike polynomials is nearly constant. At the opposite, the noise propagation of the Shack-Hartmann WFS depends on Zernike polynomial number with a $(n+1)^{-}2$ law. In fact, the phase diversity WFS indirectly measures the phase, while the other WFS meausure a phase derivative.

The phase diversity WFS behavior is based on diffraction regime. With non mono-chromatic light, a chromatic error occurs, reported in Table 1.

spectral bandwidth $\Delta\lambda$ (nm) (λ_{min} = 440 nm)	100	200	300
residual error σ_φ (λ rms)	$\frac{\lambda}{700}$	$\frac{\lambda}{350}$	$\frac{\lambda}{200}$

Tab. 1: Wavefront residual error vs spectral bandwidth

For practical implementation, a spectral filter is introduced. Its bandwidth limits the flux level and measurement accuracy. With Table 1, we can see that the spectral bandwidth is not critical in the visible domain.

Currently, the phase diversity technique is limited to phase amplitudes smaller than 2π radians. Indeed, the PSF depends on $\exp(i\varphi)$ which is defined modulo 2π. In the active optics case, the aberrations to be measured are quite small and this restriction is not a limitation.

We must also take into account the fitting and the aliasing errors. The fitting error is also given by Eq. 4.7. We have studied the aliasing error by numerical simulations and have shown that it is quite low, less than five per cent of the fitting error. Besides, we have studied the contribution of a given non reconstructed mode to the aliasing error. We have shown that its contribution decreases when its order increases[Mey 97].

4.3 - The curvature sensor

4.3.1 - Introduction

Used with point sources or limited extent sources, the curvature sensor is implemented in several adaptive optics systems[Rod 88]. It can also be used to control on-board active optical instruments. In this case, the point source is on the ground or in the instrument.

4.3.2 - Principle

This sensor was first proposed by Roddier[Rod 88]. Its principle is described in Figure 5. It consists of recording two symmetrical out-of pupil plane images. If necessary, a field lens is used for symmetry in order to reimage the pupil. A local wavefront curvature produces an excess of illumination in one plane and a lack of illumination in the other plane (Figure 5).

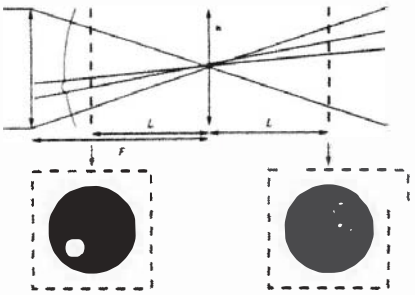

Fig. 5: Principle of the curvature wavefront sensor

In the geometrical optics approximation the difference between the two irradiance distributions may be expressed as a measurement of the local wavefront curvature inside the beam and of the wavefront radial first derivative at the edge of the beam. The measured signal is the normalized difference between the illumination $I_1(\vec{r})$ and $I_2(\vec{r})$ respectively in plane P_1 (intra focus) and P_2 (extra focus) and is given by:

$$S(\vec{r}) = \frac{I_1(\vec{r}) - I_2(-\vec{r})}{I_1(\vec{r}) + I_2(-\vec{r})} = \frac{\lambda F(F-L)}{2\pi L}\left(\frac{\delta\varphi}{\delta n}\left(\frac{F\vec{r}}{L}\right)\delta_c - \nabla^2\varphi\left(\frac{F\vec{r}}{L}\right)\right) \qquad (4.10)$$

Eq. (4.10) is deduced from the irradiance transport equation, valid for paraxial beam propagation. Therefore the diffraction effect is assumed to be negligible on the measured intensities. This condition implies that $(F-L)\Theta \leq \frac{DL}{F}$ where D is the aperture size and Θ is the angular diameter of the PSF for a point source or of the object for a limited extent source.

The wavefront reconstruction is done by solving the Poisson equation (4.10) with the appropriate boundary conditions.

Notice that the normalization by $I_1(\vec{r}) + I_2(-\vec{r})$ yields to a sensor relatively insensitive to the non-uniformity of the intensity repartition in the pupil plane.

If L is large, the difference between the two intensity distributions produced by an aberration will be smaller (Eq. 4.10) but the sampling of the wavefront can be higher than for L small.

4.3.3 - Wavefront errors

We have simulated the performance of this WFS. As an example , the signal S (Eq.4.10), obtained with a spherical aberration, is shown in Figure 6.

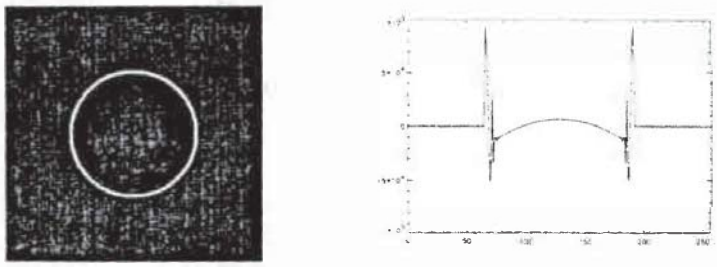

Fig. 6: curvature wavefront sensor: simulations. Signal and cross section of the signal

We have studied the influence of the sampling on the wavefront estimation. It was found empirically an optimal sampling step. It is roughly ten times the extra-focal point spread function width.

The photon noise influence on the phase measurement can be expressed by[Rou 93]:

$$\sigma_s^2 = 4\pi^2 \frac{1}{N_{ph}} \left(\frac{\Theta D}{\lambda} \right)^2 \text{(rd)}^2 \qquad (4.11)$$

N_{ph} is the number of photoelectrons per sampling point. σ_s^2 is directly proportional to L^2. This equation is similar to Eq 4.4. This demonstrates the equivalence of the signal-to-noise ratio for slope and curvature sensors. σ_ϕ^2 is proportional to N_{ph}^{-1}. When a modal reconstruction is used and for a Zernike expansion σ_{ai}^2 follows a $(n+1)^{-4}$ law.

The fitting error is the same as that given by the other WFS. The aliasing effect is important[Rou 93]. It depends on the spectrum of the aberrations of the active optical system.

Notice that the signal (eq 4.10) is not linear with respect to the aberration amplitude. This introduces a bias in the measurement.

4.3.4 - Implementation

We have proposed a curvature sensor design in order to control the wavefront on an Earth observation instrument. The measurement is done with an internal point source by auto collimation using the sight-change mirror. The two images are recorded by the same detector for compactness. The proposed design is reported in Figure 7.

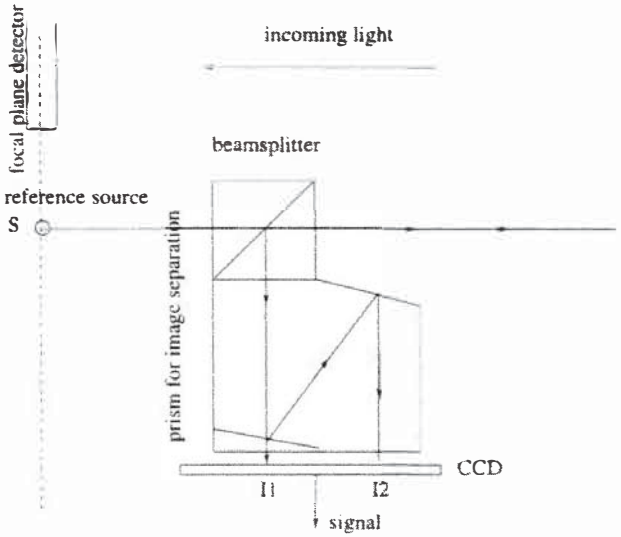

Fig. 7: curvature sensor implementation project

5 - WAVEFRONT SENSOR COMPARISON

The main properties of the three WFS are summarized in Table 2. The advantages and the disadvantages are given for using them in active optics systems. The Shack-Hartmann and the phase diversity WFS can be used with extremely extended sources. Even if the phase diversity WFS is monochromatic, it is possible to use it with quite large spectral bandwidth without noticeable degradation. The curvature WFS presents the advantage to be easily implemented with a point source. The three presented WFS are well adapted to measure low order aberrations such as those appearing with structure deformation.

SENSORS	PERFORMANCE	ADVANTAGES	DISADVANTAGES
Shack-Hartmann	- slope measurement - $\sigma_\varphi^2 \alpha \frac{1}{N_{phot}}$ - $\sigma_{a_i}^2 \alpha (n+1)^{-2}$ - aliasing error quite low	- geometrical optics (white light extended sources usable) - extended sources usable - high order aberrations	- requires additional optics - possible misalignment and need of calibration
Curvature sensor	- curvature measurements - $\sigma_\varphi^2 \alpha \frac{1}{N_{phot}}$ - $\sigma_{a_i}^2 \alpha (n+1)^{-4}$ - aliasing error important	- easy implementation - geometrical optics (white light, limited extent sources usable)	- use with very extended sources to be proven - non linear response
Phase diversity	- indirect phase estimation - $\sigma_\varphi^2 \alpha \frac{1}{N_{phot}}$ - $\sigma_{a_i}^2$ constant versus n - aliasing error quite low	- easy implementation - adapted to low order aberrations - extended sources usable	- diffraction ⇒ spectral bandwidth filter - time cost computation

Tab. 2: Comparison of the different WFS

To optimally design wavefront sensor, Table 3 shows which parameters of the sensor have an influence on the accuracy of the wavefront determination. As we have seen before, this accuracy depends on the noise from the measurements but also on the number of sampling points. The optimal number of these points are deduced from the type and the amplitude of the aberrations to be measured and also from the high order residual aberrations of the optical components.

sensor key parameters / WF characteristics	Shack-Hartmann	Curvature sensor	Phase diversity
aberration types	- subaperture number	- distance L (the higher L the higher aberration order)	- pixel number
aberration amplitude	- pixel number	- distance L (the higher L the higher aberration amplitude)	- must be less than 2π radians
accuracy	- flux level - subaperture number	- flux level - distance L (the smaller L the better accuracy)	- flux level - polynomial number - spectral bandwidth

Tab. 3: Wavefront sensors design

6 - CONCLUSION

In this paper, the three main wavefront sensors which can be implemented in an active optics system have been presented. Their performance have been compared. The main characteristics of their design are given, depending on the main Wavefront characteristics to be measured. The experimental validation of the performance is under way.

References

[Mal 92] D. Malacara, "Optical Shop Testing", *John Wiley & Sons, Inc., 2nd edition*, 1992.

[Fie 82] J.R. Fienup, "Phase retrieval algorithms : a comparison", *Applied Optics vol 21*, 1982, pp. 2758-2769.

[Ger 71] R.W. Gershberg, W.O. Saxton, "Phase determination from image and diffraction plane pictures in the electron microscope", *Optik vol 34*, 1971, pp. 275-283.

[Pax 92] R.G. Paxman, T.J. Schulz, J.R. Fienup, "Joint estimation of object and aberrations by using phase diversity', *JOSAA vol 9 n°7*, 1992, pp. 1072-1085.

[Fon 92] V. Michau, G. Rousset and J.C. Fontanella, 'Wavefront sensing from extended sources", *Summer Worshop*, Sunspot, New Mexico, 1992, pp. 124-128.

[Sou 80] W.H. Southwell, "Wavefront estimation from wavefront slope measurement", *JOSA vol 70 n°70*, 1980, pp. 998-1006.

[Rou 93] G. Rousset, "Wavefront sensing", *Adaptive Optics for Astronomy*, NATO ASI series vol 423, Cargèse, 1993

[Rig 92] F. Rigaut, E. Gendron, *Astron. Astrophys. 261*, 1992, pp. 677.

[Gon 82] R. A. Gonsalves, "Phase retrieval and diversity in adaptive optics", *Optical Engineering vol 21*,1982,pp 829-832.

[Rod 93] C. Roddier, and F. Roddier, "Combined approach of the Hubble Space Telescope wavefront distortions analysis",*Applied Optics vol 32*, 1993, pp. 2992-3008.

[Fie 93] J. R. Fienup, J.C. Marron, T. J. Schultz, and J. H. Seldin, "Hubble Space Telescope characterized by using phase-retrieval algorithms",*Applied Optics vol 32*, 1993, pp. 1747-1767.

[Mey 97] L. Meynadier, "Analyse de surface d'onde pour le contrôle actif d'un télescope spatial", Thèse de doctorat (in preparation), Université de Nice, Novembre 1997.

[Rod 88] F. Roddier : "Curvature sensing and compensation: a new concept in adaptive optics", *Applied Optics vol 27 n°7*, 1988, pp. 1223-1225.